

THE BEAM COLLIMATOR SYSTEM OF J-PARC RAPID CYCLING SYNCHROTRON

K. Yamamoto, Japan Atomic Energy Agency (JAEA), Tokai, Naka, Ibaraki, 319-1195 Japan

Abstract

A 3GeV Rapid-Cycling Synchrotron (RCS) in Japan Proton Accelerator Research Complex (J-PARC) has been commissioned since September 2007. The most important issue in the beam study is to reduce unnecessary beam loss and to keep the beam line clean for the sake of maintenance and upgrade of the machines. From experience of the former accelerators, the average beam loss should be kept at an order of 1 watt per meter for hands-on maintenance. Since it is very difficult to control the beam loss at such a low level, the only measure we can take is to localize any of the losses in a restricted area, where deliberate modules should be provided for quick coupling and remote handling in order to mitigate the personal doses. Accordingly, we have designed the beam collimation system for the purpose of the beam loss localization. We report the performance of the beam collimation system of RCS through the first commissioning results and the residual doses around RCS components.

INTRODUCTION

The Japan Proton Accelerator Research Complex (J-PARC) project is a joint project of Japan Atomic Energy Agency (JAEA) and High Energy Accelerator Research Organization (KEK). The accelerator complex consists of a 181MeV (at the first stage) or 400MeV (at the second stage) linac, a 3GeV Rapid-Cycling Synchrotron (RCS), and a 50GeV synchrotron Main Ring (MR) [1]. The RCS ring accelerates a proton beam up to 3GeV and supplies it to the MR and the Material and Life science experimental facility (MLF). Construction of the RCS has completed and beam commissioning have been started since September 2007 [2]. The RCS ring was designed to generate a high power proton beam of 1MW at the repetition rate of 25 Hz. In designing such high intensity accelerator, the primary concern is the radio-activation of the accelerator components caused by uncontrolled beam loss. From experience of former accelerator operation, the average beam loss should be kept at an order of 1 watt per meter for hands-on maintenance [3][4]. Since it is very difficult to control the beam loss at such a low level, the only measure we can take is to localize uncontrolled loss in a restricted area. A beam collimator system is devoted for such purpose. It must be a deliberate module which has quick connection and remote handling system in order to mitigate the personal doses. This report summarizes a design and performance of the beam collimator system of J-PARC RCS. In section 2 we present a conceptual design of the collimator system. Section 3 shows the simulation results of beam loss distribution and radiation effect. Results of some hardware developments are shown in section 4. Next section demonstrates the results of first

beam commissioning which was carried out from September 2007 to June 2008. A summary is given by section 6.

CONCEPTUAL DESIGN

A classical two-stage collimator system is applied for RCS[5][6][7]. An additional primary collimator is designed for the longitudinal collimation. The two-stage collimator system consists of a primary collimator and secondary collimators. The thin primary collimator scatters halo particles and the secondary collimators absorb those particles. The beam loss can be localized in a restricted region where the phase advance from the primary collimator is less than 180 degrees.

The transverse primary and secondary collimators are installed in the half of the injection straight section, which has dispersion-free optics design. The transverse primary collimator is made up of the horizontal and vertical scatterers, and it is put on the entrance to the collimator region. The five secondary collimators are installed downstream of the transverse primary collimator.

The longitudinal collimation system is composed of a longitudinal primary collimator and the above two-stage (transverse primary and secondary) collimator. The longitudinal primary collimator is installed in the arc section in front of the injection point. The longitudinal halo particle that is scattered by longitudinal primary collimator is diffused between the acceptance of the transverse collimators and another component. Scattered particles can pass through the vacuum pipe until it hits the transverse collimators again.

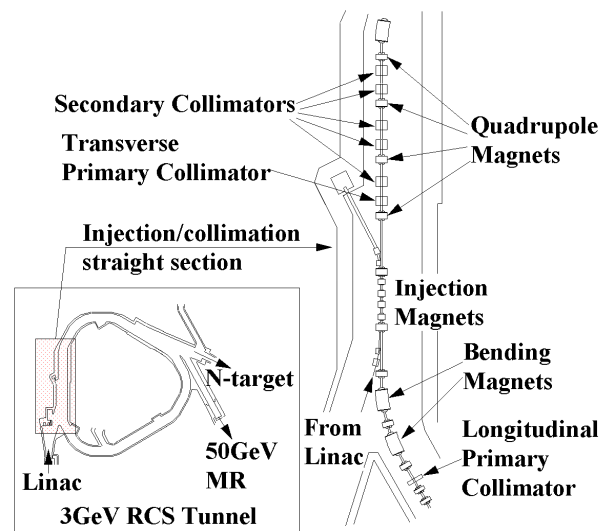


Figure 1: The location of the collimation system in the RCS.

Both primary collimators have apertures restricting emittance to $324\pi\text{mm.mrad}$ and 1% momentum deviation. All secondary collimator apertures are set at $400\pi\text{mm.mrad}$. These values are set to prevent the beam from reaching the secondary collimator before halo particles hit the primary collimator. All of the other vacuum chambers are designed for a beam with more than $486\pi\text{mm.mrad}$ emittance and 1% momentum deviation. Figure 1 shows the location of the collimation system in the RCS, and the twiss parameters of the RCS are shown in Figure 2.

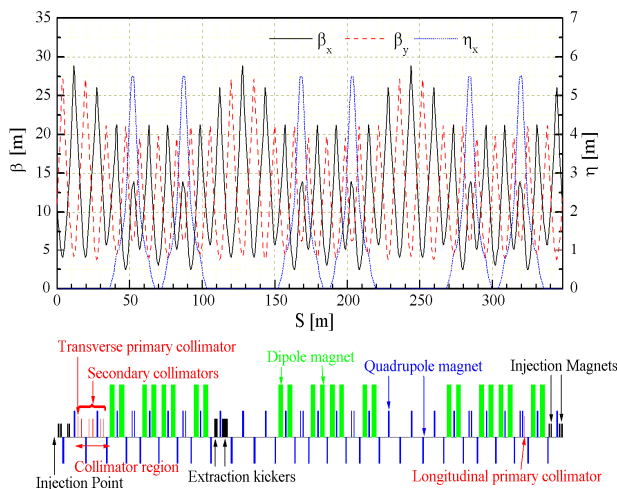


Figure 2: The location of the collimation system in the RCS.

The transverse primary collimator and each secondary collimator are made up of 4 direction plates (upper, lower, right and left). The longitudinal primary collimator is made up of horizontal 2 plates (right and left). Height and width of these plates are $100\text{mm} \times 100\text{mm}$. The material of the transverse primary collimator is tungsten, and its thickness is 1mm. The material of the longitudinal primary collimator is graphite sheet and it is 0.1mm in thickness. These materials are chosen for their availability and high melting point. These thicknesses are decided from the necessary scattering angle of particles. The secondary collimator plates are made of copper. Their thickness are 200mm. This value is chosen so that several hundreds of MeV protons can be stopped. The material of the secondary collimator is chosen for high density and high thermal conductivity in order to release heat from energy deposition. All collimator plates (Transverse, longitudinal primaries and all secondary collimators) can be moved independently.

SIMULATION

Simulation of Beam Loss Distribution

We estimated the performance of the RCS collimator system under various conditions. The beam loss distributions were calculated by the STRUCT code[8].

The STRUCT was developed at Fermi National Accelerator Laboratory. It calculates a beam track and a scattering effect. In order to calculate the beam loss distributions, we assumed two types of particle distributions in the transverse and longitudinal phase space. The one is a transverse halo distribution, and the other is a longitudinal halo distribution. Transverse halo is distributed from $324\pi\text{mm-mrad}$. to $344\pi\text{mm-mrad}$. emittance and its momentum is distributed from -1% to 1%. Longitudinal halo spreads out in 1% to 1.1% of range in the absolute momentum value and transverse emittance is from $0\pi\text{mm-mrad}$. to $324\pi\text{mm-mrad}$. All calculation models assumed that the beam energy was 400MeV and the amount of total beam loss was 4kW. In these calculations, we defined the collimation efficiency as follows:

$$\text{Collimation efficiency} = \frac{\text{beam loss [W] in the Collimator region}}{\text{beam loss [W] in whole ring}}$$

This value is an indicator of collimation performance. An example of the beam loss distribution is shown in Figure 3. In this case we assumed that transverse halo collimation was done at the nominal operation point ($v_x=6.68$, $v_y=6.27$) without any errors. As a result, collimation efficiency is about 98% and 1 W/m criterion was almost cleared. The maximum loss power at one collimator is 1.2kW at first secondary collimator and the maximum heat load on one plate is 540W.

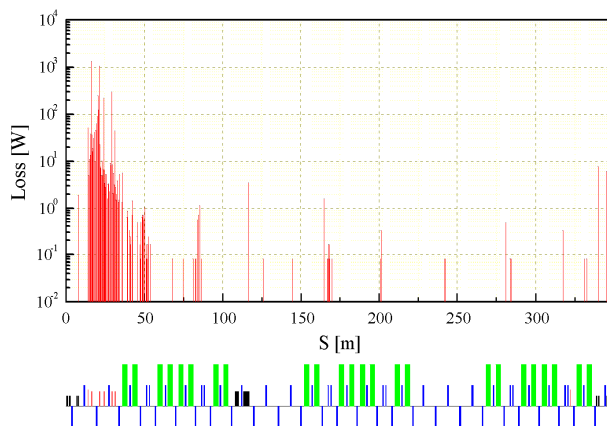


Figure 3: Schematic of J-PARC RCS collimator.

Estimation of Residual Dose

In order to develop the RCS collimator system, next we calculated the radiation dose of the collimator and decided necessary shield thickness. We must suppress the residual dose less than 1 W/m level at the outside of the shielding wall. The estimation of the radiation dose and the radiation shielding design of collimator were carried out by the MARS code[9]. The MARS was also developed at Fermi National Accelerator Laboratory. In

order to estimate the radiation dose from the collimator, we made the following model : the collimator vacuum chamber was covered with the 300mm iron inner shield and the 800mm concrete outer shield. From the simulation result of the STRUCT, the maximum loss power was estimated about 1.2kW at 400MeV. The MARS calculation result is shown in Figure 4. This result indicates the residual dose distribution of the collimator

and its shielding after 1 month operation and 1day cooling. In this result, the collimator copper block is activated over 1Sv/h, but the surface of the outer concrete shield is activated over 1Sv/h, but the surface of the outer concrete shield is activated mostly under 1mSv/h and this value is almost same as the residual dose rate of the 1W/m region. The personal dose by the collimator can suppress by this shielding. The residual dose of whole RCS tunnel was calculated by Nakao et al[10][11].

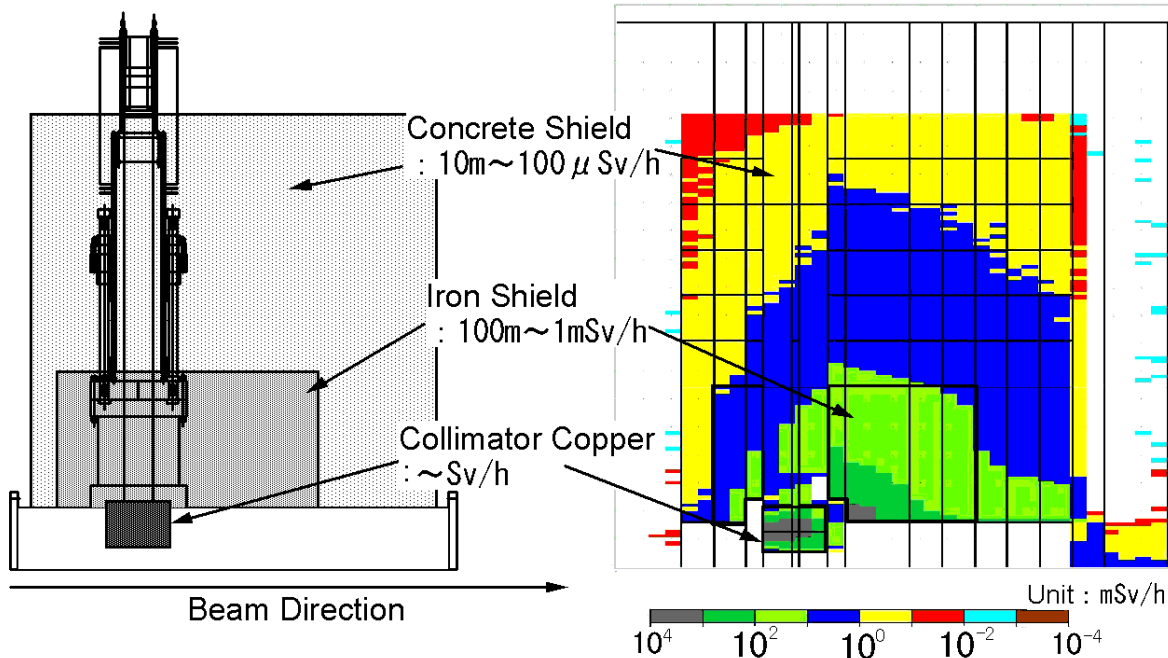


Figure 4: Estimation of the Residual Dose. This is the side cross section of collimator shield. Residual dose rate [mSv/h] is distinguished by colours. The collimator is drawn a dark green and grey and it means there are over 1mSv/h residual dose. The surface of the outer concrete shield is almost yellow and it means there are under 1mSv/h residual dose.

HARDWARE R&D RESULTS

Since the collimator system suffers a large amount of radiation, we studied reliability and feasibility of all collimator components. Figure 5 shows the R&D items of collimator components.

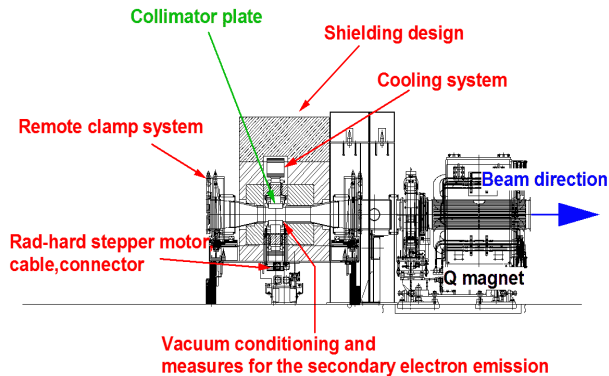


Figure 5: Schematic of J-PARC RCS collimator.

Gamma-Ray Irradiation Test

We carried out the gamma-ray irradiation test by the Co-60 gamma-ray source[12][13]. Each component was developed and checked its radiation durability. Especially we developed a new stepper motor which had high durability more than 100MGy absorbed dose.

Cooling System

In order to avoid an accident by cooling water, we use an air cooling system of the thermal conductor. From the STRUCT result, the maximum loss per one plate was assumed as 700Watt (this includes 160W margin). Figure 6 shows the result of the ANSYS simulation at the maximum calorific values. The simulation result shows that the collimator temperature can be kept less than 130 degrees centigrade with the copper conductor of 140mm diameter by natural air cooling.

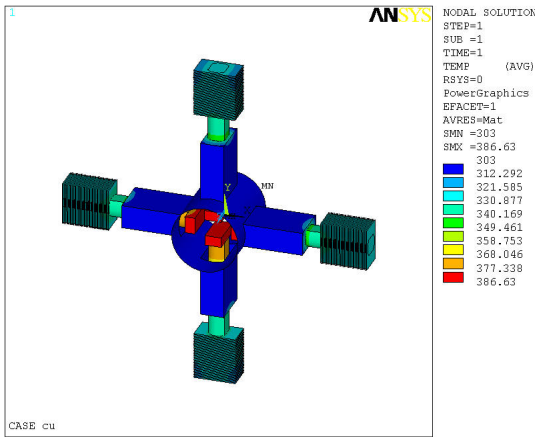


Figure 6: Schematic of J-PARC RCS collimator.

We tested the cooling capacity of this system by using the R&D machine. The experiment was carried out in the vacuum of less than 10^{-4} Pa. The heater was installed in the vacuum chamber and attached collimator plate. As a result, the temperature exceeded 200 degrees C with the

design heat (700W) by natural air cooling. Next we tried forced air cooling by using the cooling fan and the temperature of the horizontal collimator fell below 120 degrees C. We adopt forced air cooling system[14].

Remote Clamp System

By using the remote clamp system, the collimator vacuum flange can be connected/detached by merely turning a screw in a place away from the collimator. The quick-coupling clamp can be opened/closed by turning two screws that are connected with the clamp, and another screw separate/close the flange of collimator chamber and the flange of other accelerator component. The rotational number and the torque of all the screws are controlled by the nut runner, which is set by the crane. The clamp closing system is shown in Figure 7. After confirming all action, we checked by the helium leak examination that it can close less than $5.0E-10$ Pa m³/sec helium leak. Moreover, it was confirmed that the leak level was same even if the central axis of opposite flanges was off to the side as 1mm[14].

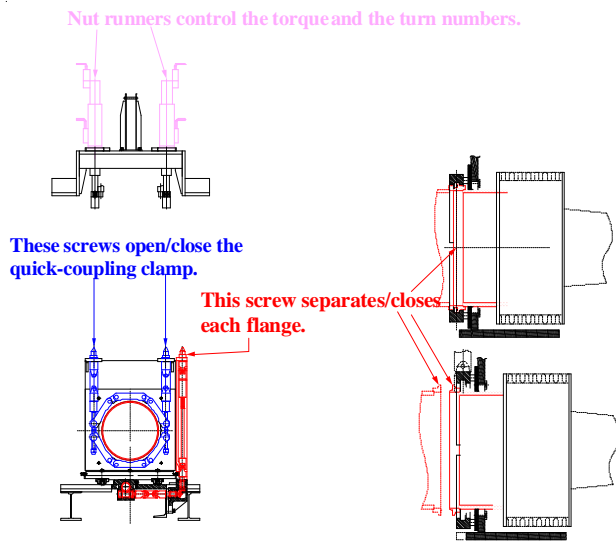


Figure 7: Schematic of the remote clamp system. By using the remote clamp system, the collimator vacuum chamber can be removed only by turning the screws far from the collimator. The quick-coupling clamp can be opened by turning two screws which are connected with the clamp, and the other screw separates the flange of collimator chamber and the flange of other accelerator component.

Surface Coating and Vacuum Treatment

Since the radiation from the collimators will become the source of the secondary electrons, there is a possibility of bringing about the beam instability by those secondary electron clouds[15][16]. In order to reduce these undesirable electron emission, the Titanium Nitride (TiN) is coated on the inside surface of the chamber and the collimator copper block. We measured the secondary

electron yield (SEY) from the TiN film with various condition[17] and it was enough lower level.

Vacuum treatment of collimator component is also important. All components were prebaked more than 450degrees C. when those were still ingredients. All inner surface of vacuum chamber was electro-chemical polished before coating. Whole collimator system was baked more than 150degrees C. at final stage of assembly.

FIRST BEAM COMMISSIONING RESULT

Beam Loss Monitor Signals

The first beam commissioning period had been started since September 2007 and finished June 2008. We had two aims during the first beam commissioning. The first one is to establish a stable 4kW beam acceleration for MR and MLF, and the other is to achieve higher intensity as possible. In the early stage of the beam commissioning, the full beam loss of several shots have occurred along the ring owing to the insufficient adjustment of the beam monitors or wiring mistake of the magnet. But those problems were solved immediately and the beam acceleration was established. However, the beam loss have still occurred in the following points.

- (1) The junction point of L3BT injection beam and RCS circulating beam.
- (2) The upstream entrance of the transverse primary collimator chamber.
- (3) The branch of H0 dump line.
- (4) The branch of extraction line.
- (5) The transverse collimators
- (6) Dispersion maximum points in the arcs

Beam Loss Monitor (BLM) signals at these points are shown in Figure 8. The BLM signal at loss point (2) is shown in Figure 8(a). The BLM of Figure 8(b) was put at the branch of H0 dump line (point (3)), BLM of Figure 8(c) was put outside of shielding wall around the first secondary collimator (point (5)), and BLM of Figure 8(d) was put at a dispersion maximum point in the arc (point (6)).

The beam loss at the injection junction point (point (1)) was thought that it was caused by the pressure rise due to cracks of a ceramic duct. This ceramic duct was set in the quadrupole magnet close to injection junction. The beam loss signal was no longer detected after replacement of broken ceramic duct.

The beam loss signal at the upstream entrance of the transverse primary collimator chamber (point (2)) was distinctive. In this study, the shift bump magnets (which make a bump orbit in order to merge injection beam and circulating beam) were excited during 500 μ sec. The BLM signal increased since a beam injection was started (from 100 μ sec), and signal peak has continued till 600 μ sec when a bump orbit began to fall. Finally BLM signals disappeared while a bump orbit has completely fallen. From this result, it was thought that this loss was caused by multiple scattering between a charge exchange foil and circulating beam which brought close to a foil by the bump excitation (see Figure 8(a)).

At the branch point of H0 dump line (point (3)), the beam loss was caused by the same reason above point (2). In addition, the beam loss of this point was also affected by the circulating beam during acceleration period (see Figure 8(b)).

The loss signal near an extraction line (point (4)) disappeared with adjustment of C.O.D. and extraction orbit.

The beam losses at transverse collimators (point (5)) were the "controlled" loss. The beam loss occurred during injection process and the middle phase of acceleration period (see Figure 8(c)).

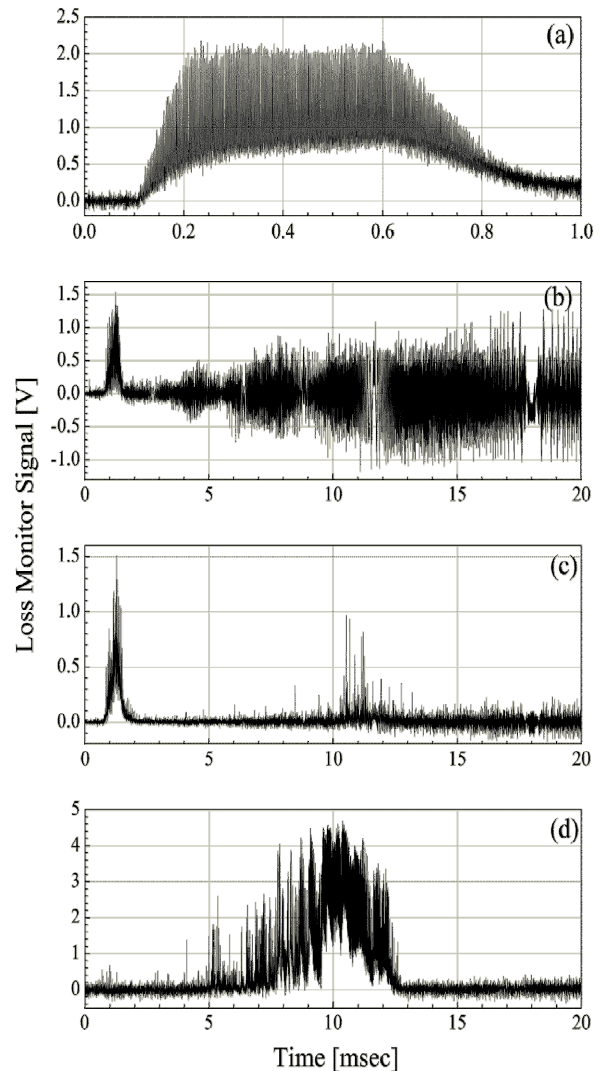


Figure 8: BLM signals. Vertical axis means the voltage from BLM. Input impedance of preamp is 50 Ω , HV bias voltage is -1550V (P-BLM) and -600V (S-BLM). Each signal was 1000 multiplied by the preamp which was located at sub-tunnel. Horizontal axis is measurement time from injection. Figure 7 (a) is a signal during 1msec of injection period. Figure 7 (b)-(d) are signals during acceleration period.

The loss occurred near the dispersion maximum point in the arc (point (6)) when the longitudinal halo leaked from the RF bucket. Since only ten of eleven sets of RF cavities are installed at present, the beam loss occurs near 10msec while requirement of cavity voltage becomes the highest. But there was no longitudinal loss in usual operation. The loss at the arc was occurred only during the RF parameter search.

Beam Current

The number of particles correspond to about 50kW per bunch (4.3×10^{12}) was accelerated in the latest study of the first beam commissioning. The number of particles measured by Wall current monitor and DC Current Transformer is shown in figure 9. The painting bump did not use and all injection beam have entered into the ring center orbit in piles. In this study, the loss during the acceleration period was 3.4%. It has occurred during 2 msec after injection start, and most of lost particles were absorbed with the collimators.

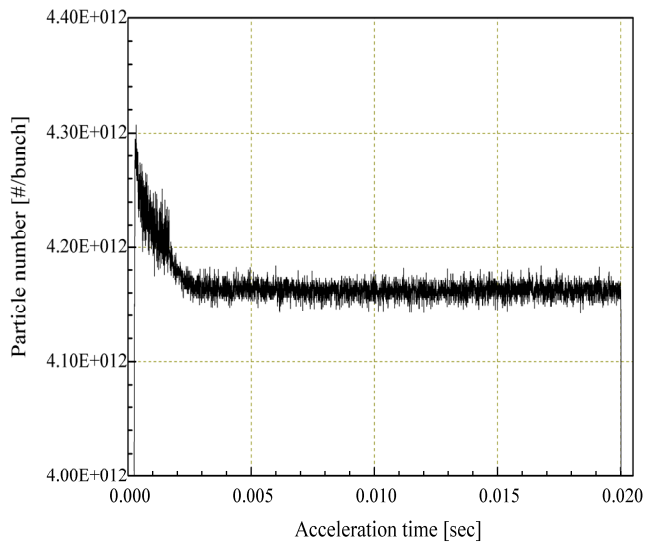


Figure 9: Particle number during acceleration.

Residual Dose Rate After Beam Study

The amount of residual dose is shown in Figure 10. These values were immediately measured after the end of beam study on June. The beam condition was that the 4kW beam was provided to the MLF and MR during day time of one week and 100kW beam test was rarely carried out.

From this residual dose result, the above-mentioned loss of point (2) and point (3) should be especially taken care. The residual doses of $380 \mu\text{Sv/hr}$ have been generated by the loss of point (3) and $140 \mu\text{Sv/hr}$ has been generated by the loss of point (2).

Practically, each collimator would have much larger residual dose. But the collimator chambers were covered with thick shielding wall and we could not measure the inside of the collimator shielding. We could detect only the residual dose on the outside of shielding and it is a background level.

Acceptance Ratio of Primary to Secondary Collimator

We investigate the effect of the acceptance ratio of the transverse primary to secondary collimator. Figure 11 shows the BLM signal at the first dispersion maximum point after the collimator region. At first we set the collimator acceptance as designed value : Primary is $324\pi\text{mm-mrad}$. and Secondary is $400\pi\text{mm-mrad}$. and there was no significant loss. Next we reduced only primary acceptance as $200\pi\text{mm-mrad}$. Then some loss signals appeared. Finally we reduced both primary and secondary, and the loss signals disappeared again. It seems that the unbalanced acceptance ratio caused leakage loss from collimator region. Designed acceptance has enough performance

Longitudinal Collimation

We checked the longitudinal collimator performance during the study of the RF parameters. When the longitudinal halo was lost at the dispersion maximum point, we inserted the longitudinal primary collimator. Then some loss were lead on the transverse secondary collimators, but BLM signal of the dispersion maximum point was scarcely reduced. So the longitudinal collimator did not work our expectation. We think the reason is that the longitudinal primary collimator was optimized to the collimation at injection energy. The scattering angle of the accelerated proton was not enough to increase as necessary size for transverse collimation. Furthermore, we did not use the painting injection and the beam size was very small. Therefore, the longitudinal primary collimator could not lead the longitudinal halo on the transverse collimators.

Fortunately, there was no longitudinal halo in usual operation at present because of good performance of the ring RF system and the Linac chopper. It is not problem as yet.

Beam Stop 30th Jun., 2008 at 12:19
 Measurement 1st Jul., 2008 at 10:30

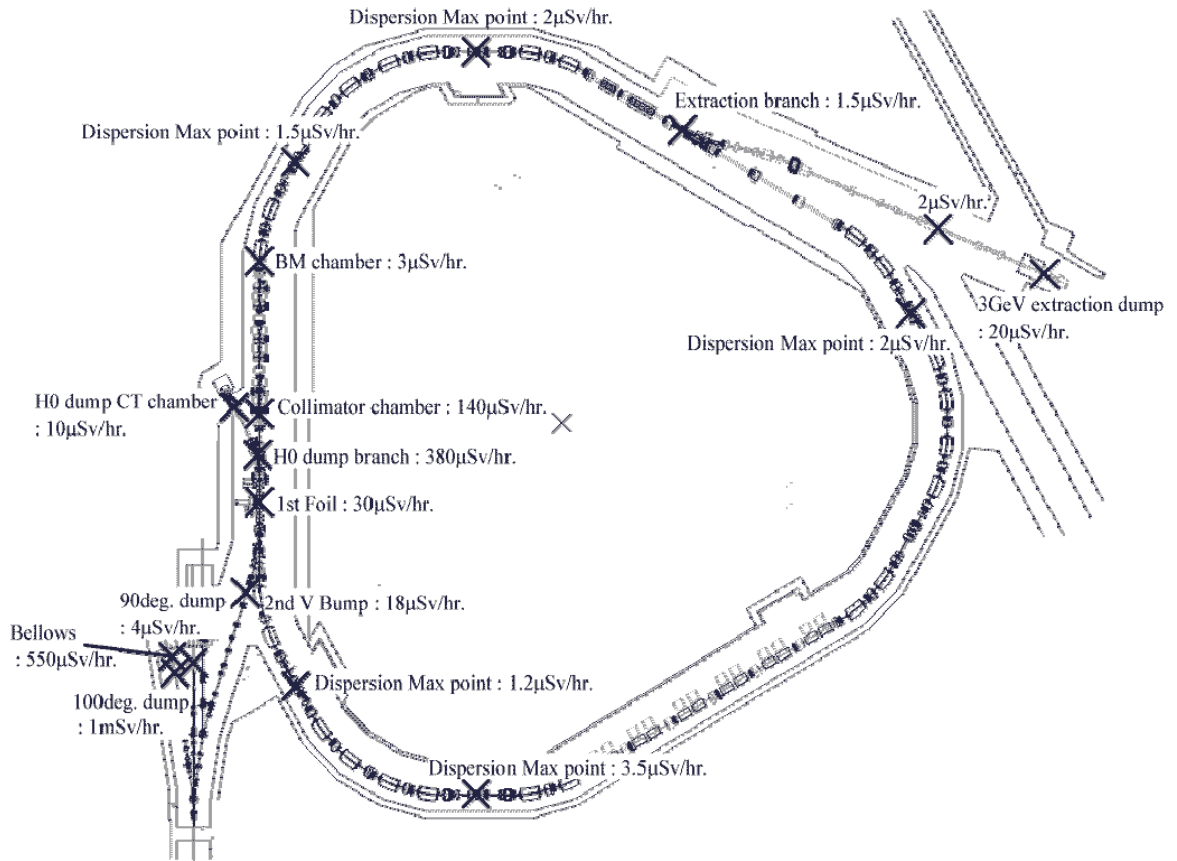


Figure 10: Example of a full-width figure showing the distribution of problems commonly encountered during paper processing. This figure is labeled with a multi-line caption which has to be justified, rather than centred.

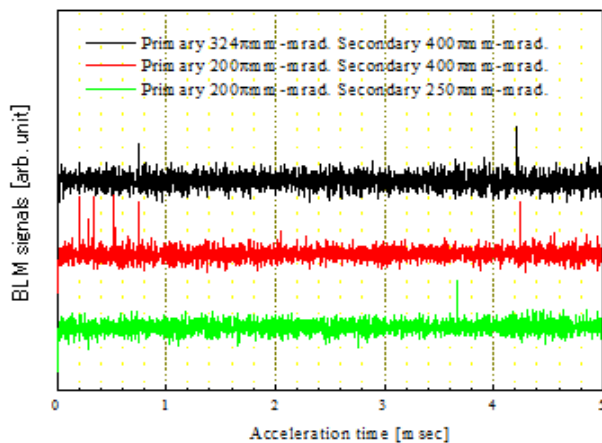


Figure 11: Particle number during acceleration.

CONCLUSION

We succeeded in establishing stable 4kW beam supply for MR and MLF and demonstrating 100kW high intensity operation. It is remarkable that there were rarely high residual dose point after demonstration of the 100kW operation. This was due to the good performance of all RCS components, especially the collimation system had enough performance. It can remove almost the transverse halo. On the other hand, longitudinal collimation system needs more improvement. Fortunately, there was no longitudinal halo during less than 100kW operation so far. We will further study of the beam collimator system in order to achieve higher beam intensity.

REFERENCES

[1] Y. Yamazaki, *et al*, Accelerator Technical Design Repor for High-Intensity Proton Accelerator Facility Project, J-PARC, KEK-Report 2002-13; JAERI-Tech 2003-044.

- [2] H.Hotch, "Status of J=PARC commissioning", Proc. 42nd ICFA Advanced beam dynamics workshop HB2008 (2008).
- [3] N.Mokhov and W.Chou *et al*, "Beam Halo and Scraping", the report of the 7th ICFA Mini-workshop, Lake Como, Wisconsin, 1999.
- [4] JHP Project Office, "JHF ACCELERATOR DESIGN STUDY REPORT", KEK Report 97-16, JHF-97-10, March 1998.
- [5] T.Trenkler and J.B.Jeanneret, Part. Accel. **50**, 287 (1995).
- [6] J.B.Jeanneret, Phys. Rev. Special Topics-Accelerators and Beams, **1**, 081001 (1998).
- [7] P.J.Bryant, CERN Accelerator School: 5th General accelerator physics course, CERN 94-01, **1**, 159 (1994).
- [8] A.Drozhdin and N. V. Mokhov, "The STRUCT Program User's Reference Manual", SSCL-MAN-0034 (1994).
- [9] N.V.Mokhov, "The MARS Code System User's Guide Version 13(95)", FERMLAB-FN-628 (1995).
- [10] N.Nakao, N.V.Mokhov, K.Yamamoto, Y.Irie, and A.Drozhdin, "MARS14 Shielding Calculations for the J-PARC 3 GeV RCS", KEK Report 2004-1 (2004).
- [11] N.Nakao, N.V.Mokhov, K.Yamamoto, Y. Irie and A. Drozhdin, Radiation Protection Dosimetry, **116**, No.1-4, 85 (2005).
- [12] M. Kinsho *et al*, "Gamma-ray irradiation experiments of collimator key components for the 3GeV-RCS of J-PARC" in this conference.
- [13] K.Yamamoto *et al.*, "Development of the collimator system for the 3GeV rapid cycling synchrotron", Proc. PAC05 (2005).
- [14] K.Yamamoto *et al.*, "Beam collimator design for the 3GeV synchrotron of the JAERI-KEK joint project", Proc. PAC01 (2001).
- [15] T.Toyama *et al.*, Proc. the 31st ICFA Advanced Beam Dynamics Workshop on Electron-Cloud Effects "E-CLOUD'04"(2004).
- [16] K.Ohmi, T.Toyama and C.Ohmori, Phys. Rev. Special Topics-Accelerators and Beams, **5**, 114402 (2002).
- [17] K. Yamamoto, T. Shibata, N. Ogiwara, M. Kinsho, "Secondary Electron Emission Yields from the J-PARC RCS Vacuum Components", Vacuum, **81**, 788 (2007).